Scientific Journal of Impact Factor(SJIF): 3.134
e-ISSN(O): 2348-4470
p-ISSN(P): 2348-6406

International Journal of Advance Engineering and Research Development

Volume 2,Issue 3, March -2015

Performance and QoS analysis of WIMAX With Alamouti STC and MIMO

Harpreet Nijjer[1], Sandeep Kumar[2]

[1] *(M.Tech Scholar) ,Electronics & Communication Engineering, PCET, Lalru Mandi,Mohali, India*
[2]*(A.P.),Electronics & Communication Engineering, PCET, Lalru Mandi,Mohali, India*

Abstract— *WiMAX is a wireless technology that provides broadband data at rates over 3 bits/second/Hz. In order to increase the range and reliability of WiMAX systems, the IEEE 802.16-2004 standard supports optional multiple-antenna techniques such as Alamouti Space-Time Coding (STC), Adaptive Antenna Systems (AAS) and Multiple-Input Multiple-Output (MIMO) systems. In this paper, we focus on techniques that do not require channel knowledge at the transmitter, which include both Alamouti SFC and MIMO.*

Keywords— *WiMAX ,SFC, MIMO, ALAMOUTI, INTERLEAVED*

I. INTRODUCTION

WiMAX is a technology for "wireless" broadband. Wimax (Worldwide Interoperability for Microwave Access), an evolving standard for point-to-multipoint wireless networking, works for the "last mile" in the same way that Wi-Fi "hotspots" work for the last one hundred feet of networking within a building or a home. It has a number of other applications in hotspots, cellular backhaul and in high-speed enterprise connectivity.

The ability to provide these broadband connections wirelessly, without laying wire or cable in the ground, greatly lowers the cost to provide these services. So, WiMAX may change the economics for any place where the cost of laying or upgrading landlines to broadband capacity is prohibitively expensive, as in emerging countries. WIMAX technology deployment a reality for practical applications in our everyday life.

Broadband data services, such as delivery of rich Internet Protocol and media content, are an increasingly important component of the services and revenue of network operators, who want to expand the reach of their broadband data networks without expensive construction and infrastructure costs.

The technology enables long-distance wireless connections with speeds up to 75 megabits per second. However, network planning assumes a WiMAX base station installation will cover the same area as cellular base stations do today. Wireless WANs based on WiMAX technology cover a much greater distance than Wireless Local Area Networks (WLAN), connecting buildings to one another over a broad geographic area.

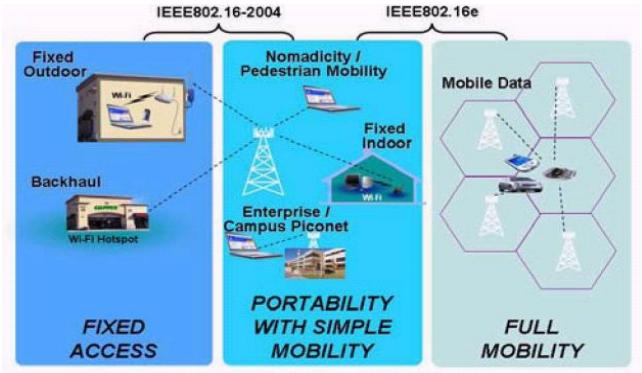

Fig1: Broadband Wireless Deployment Scenarios

This usage enhancement over fixed access requires enhancements to security such as strong mutual authentication between user/client devices. A common centralized mechanism for user authentication is needed as users may move between different APs within an IP prefix or subnet, or across APs in different subnets, or roam to other service providers in different locales. Portability with simple mobility, describes a more automated management of IP connections. It doesn't provide adequate handover performance for delay and packet loss sensitive real-time applications such as VoIP.

In fully mobile scenario, users may be moving while simultaneously engaged in broadband data access or multimedia streaming session. The need to support low latency and low packet loss handovers of data streams as users transition from one AP to another is clearly a challenging task.

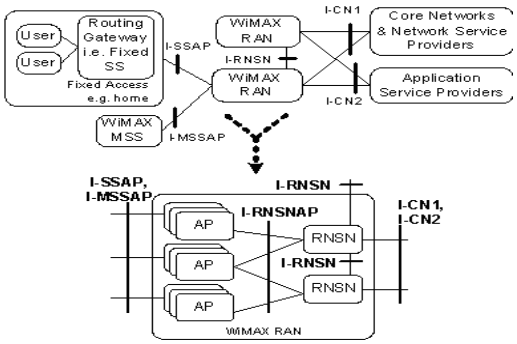

Fig2:End to End Reference Architecture

Figure2 depicts an end-to-end reference architecture for 802.16. Various functional entities and interoperability interfaces are identified. The network essentially decomposes into three major functional aggregations: the 802.16 SS/MSS, the 802.16 RAN, and interconnect to various operators IP core and application provider networks. The IP core network a) manages the resources of the 802.16 RAN, and b) provides core network services such as address management, authentication, service authorization, and provisioning for 802.16 SS/MSSs. Formatting.

In the sections below, we describe three logical entities: the Radio Network Serving Node (RNSN), AP, and SS/MSS. We also briefly describe the interoperability interfaces identified in Figure3.

A Radio Network Service Node (RNSN) is a logical network entity that interfaces the RAN with the operator IP core network, Application Service Provider (ASP) networks, and other service networks.

An 802.16 Access Point is a logical entity that provides the necessary over-the-air standards-compliant functionality including SS/MSS admission control and all RRM and UL/DL scheduling. We envision a number of AP/RAN topologies as depicted in Figure3.

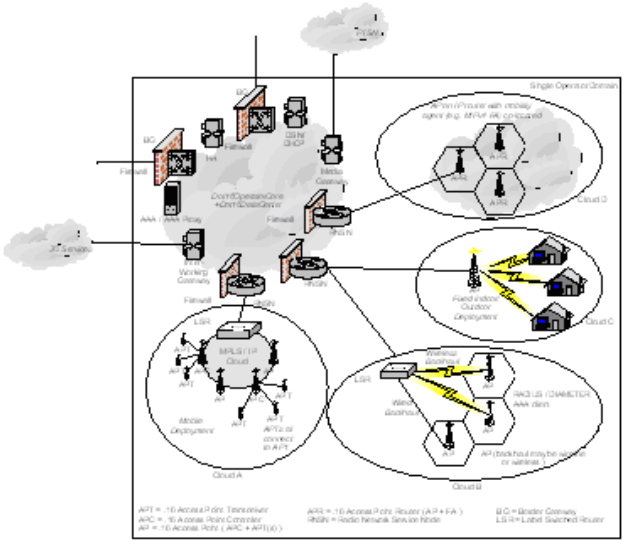

Fig3: ORTHOGONAL FREQUENCY DIVISION MULTIPLEXING

Orthogonal frequency division multiplexing (OFDM) is a multi-carrier transmission technique for high speed bi-directional wireless data communication. OFDM effectively squeezes multiple modulated carriers tightly together, reducing the required bandwidth but keeping the modulated signals orthogonal so they do not interfere with each other. It is based on frequency division multiplexing (FDM), which is a technology that uses multiple frequencies to simultaneously transmit multiple signals in parallel. Each signal has its own frequency range (subcarrier) which is then modulated by data.

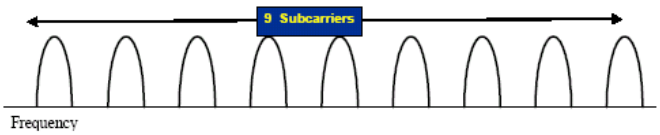

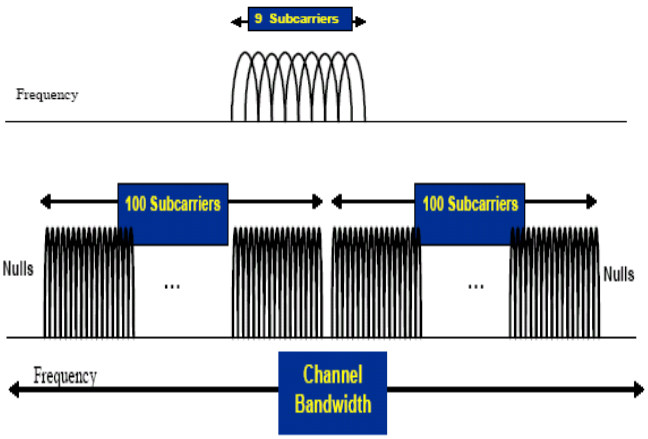

Fig4:MULTIPLE ANTENNA TECHNOLOGY SYSTEM DESCRIPTION

In order to increase the range and reliability of WiMAX systems, the IEEE 802.16-2004 standard supports optional multiple-antenna techniques. A wireless environment suffers from multipath propagation. Multipath propagation, also known simply as multipath, is a condition where multiple reflections of the transmitter waveform arrive at the receiver at different times. This is shown in Figure, where a and b are the gains of the paths and τ1 and τ2 are the delays. The reflected path is actually the sum of multiple reflections from the obstruction, which causes fading. Multipath propagation induces Inter-Symbol Interference (ISI) which is traditionally compensated for by equalizers in single carrier systems.

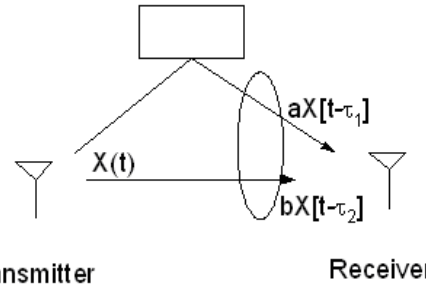

OFDM is preferable in multipath propagation scenarios. A block diagram of OFDM is shown. As long as the CP, or Cyclic Prefix, is longer than the difference in multipath propagation arrival times, or multipath spread, an equalizer is not needed.

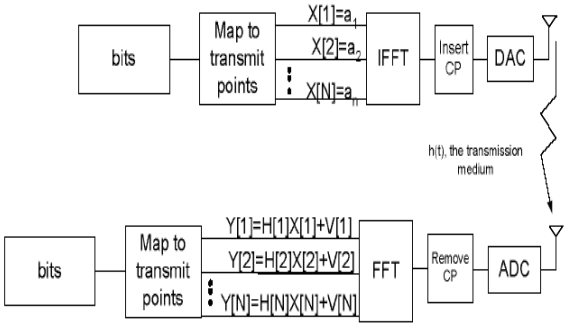

Fig5:MIMO system without Noise

Consider a MIMO system without noise as shown in Figure. In this figure, each ray corresponds to a multipath propagation channel. From the point of view of a subcarrier, each multipath propagation channel collapses to a single scalar tap. For subcarrier k, this can be expressed as shown:

$$\begin{bmatrix} Y_1[k] \\ Y_2[k] \\ Y_3[k] \end{bmatrix} = \begin{bmatrix} H_{11}[k] & H_{12}[k] \\ H_{21}[k] & H_{22}[k] \\ H_{31}[k] & H_{32}[k] \end{bmatrix} * \begin{bmatrix} X_1[k] \\ X_2[k] \end{bmatrix}$$

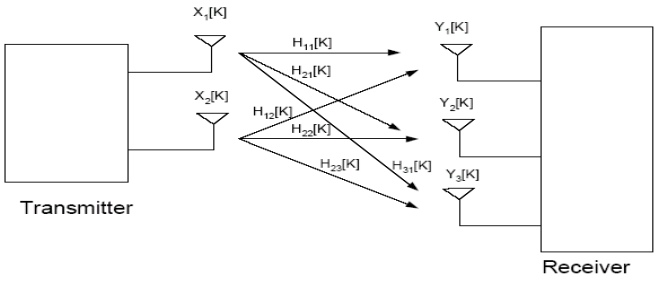

Fig6:OFDM MIMO System

In Figure, Yi[k] is the kth subcarrier output for receive antenna i, H ij[k] is the kth subcarrier gain from the jth transmit antenna to the ith receive antenna, and Xj[k] is the kth subcarrier input from antenna j. Without loss of generality, rewriting the above equation, for an OFDM system would be

$$\underline{Y} = H * \underline{X} + \underline{N}$$

where Y, H, and X are the appropriate generalizations of the 2 transmit * 3 receive antenna system and N is the noise and interference.

ALAMOUTI TRANSMISSION

The Alamouti transmission scheme is an STC in that it sends information on two transmit antennas and consists of two consecutive transmissions in time. Hence it transmits information in space and time.

$$C_1{}^*[k]Y_1[k] + C_2[k]Y_2{}^*[k] =$$
$$(\| C_1[k] \|^2 + \| C_2[k] \|^2)\hat{S}_1[k] +$$
$$C_1{}^*[k]V_1[k] + C_2[k]V_2{}^*[k]$$

$$C_2{}^*[k]Y_1[k] - C_1[k]Y_2{}^*[k] =$$
$$(\| C_1[k] \|^2 + \| C_2[k] \|^2)\hat{S}_2[k] +$$
$$C_2{}^*[k]V_1[k] - C_1[k]V_2{}^*[k]$$

Simulation and Results

MIMO Transmitter: Space-Frequency Interleaving :

Space-frequency interleaving is a simple way to provide diversity gain to a spatially multiplexed, coded data stream. This method is not currently standard-compliant. The block diagram for the Space-Frequency Interleaver (SFI) transmitter and receiver is illustrated in Figure 6. Information bits are first encoded by a Forward Error Correction (FEC) encoder, which is a concatenation of Reed-Solomon and convolutional encoders in OFDM-256 IEEE 802.16-2004. After puncturing, the binary coded bits are sent to an SFI, which maps bits to antennas and tones so as to exploit full diversity in both space and frequency. The interleaved bits are then mapped to Gray coded QAM data symbols. The receiver uses the MMSE receiver, and it sends the soft bits into the concatenated convolutional and Reed Solomon decoders.

Details of the interleaver design are available in [12]. We provide a short description here. Let q be the number of bits per QAM symbol, assume 192 data tones (256 point FFT with 64 guard tones+pilots) and M transmit antennas. The interleaver consists of three steps: (1) serial-to-parallel multiplexing of incoming q*192*M bits to M antennas, (2) IEEE 802.16-2004 interleaving on each antenna, and (3) forward circular shift of the bits on each antenna by q*cts, where cts = "cyclic tone shift" is a parameter that must be optimized for each data mode and MIMO configuration.

1 2 3 ..	1 3 5 ..	384 362 364 ...
13 14 15	25 27 29	2 4 6
25 26 27	49 51 53	26 28 30
37 38 39	73 75 77	50 52 54
:	:	:

Figure 7: IEEE 802.16-2004 bit interleaver BPSK, SF interleaver for 2x2 MIMO on antenna 1 and on antenna 2

In Figure 7 bits are mapped to tones column-by-column. Therefore bits indexed by 1, 13, 25, 37, … are mapped to tones 1, 2, 3, 4, ….etc. Our proposed interleavers are shown in the second two boxes of Figure 7.

Simulation results for this interleaver with BPSK, rate ½, 192 data tones are shown in Figure 9. SUI-3 channel models without spatial correlation are used throughout this section.

Also shown for reference is a simpler interleaver labeled SM, which does not interleave bits across antennas. Instead, it takes contiguous blocks of q*192 bits and maps them to antennas, followed by IEEE 802.16-2004 interleaving on each antenna.

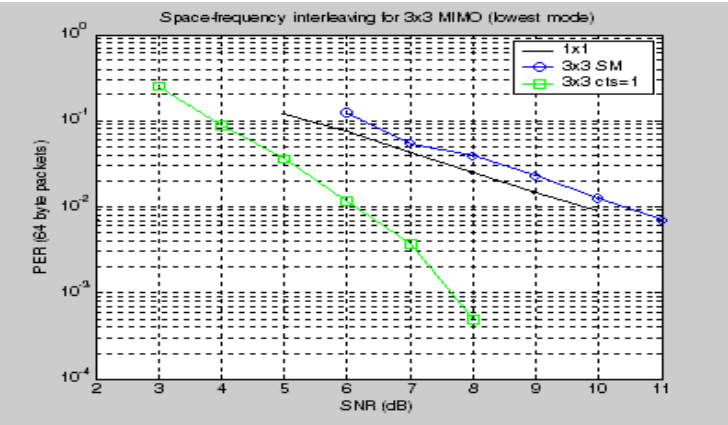

Fig8: ***SFI for 3x3 MIMO (lowest mode)***

Our interleaver provides gains of 2 to 4 dB over this simple interleaver because it has been designed to extract maximal space-frequency diversity.

At the highest IEEE 802.16-2004 mode with 64-QAM, rate ¾ coding, gains with the interleaver are not as high, but still significant at 1 to 2 dB over SM, as shown in Figure 10.

Figure 9 shows two values of cts: cts=1 and cts=64. Performance of the MMSE receiver is sensitive to the choice of cts, although cts=1 works well for most modes, channel conditions, and MIMO architectures. Performance of the ML receiver is not sensitive to the choice of cts (not shown here).

This suggests that the MMSE receiver induces correlation across space-frequency blocks. The MMSE induces correlation across antennas because of cross-talk, and the channel induces correlation across tones because of limited delay spread. A combination ends up correlating adjacent tones on all antennas. The proposed interleaver places bits on uncorrelated tones and antennas, thereby improving performance with the MMSE receiver.

Figure 9 also shows performance with an SVD receiver, which requires channel feedback to the transmitter in order to diagonalize the channel matrix.

Note in Figures 8 and 9 that the 3x3 architectures fall short of 1x1 by 3 to 5 dB. Therefore these MMSE-MIMO architectures do not maintain range at the higher throughputs.

Advanced receivers are required to improve range at high rates, and they are the subject of the next sub-section.

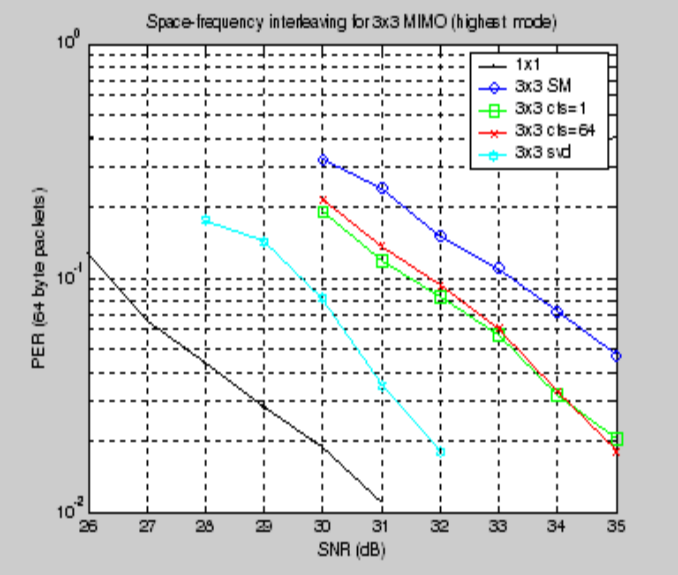

Fig 9: ***SFI for 3x3 MIMO at highest mode***

MIMO Advanced Receivers: Iterative Decoding

A non-iterative receiver similar to that used in the previous sub-section is shown in Figure 10.

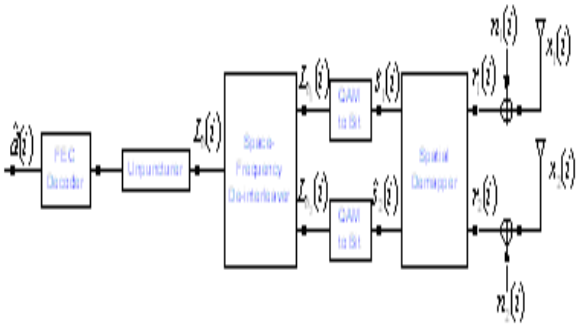

Figure 10: ***Illustration of non-iterative receiver***

The spatial demapper above decouples the data streams mixed by the channel matrix over the air. The MAP demapper has the best performance and the highest complexity, while linear demappers such as MMSE and ZF have low complexity but poor performance compared to MAP. Recently, techniques such as sphere decoding have been proposed to reduce the complexity of MAP receivers.

After the spatial streams are separated, the "QAM to bit" functional block converts the noisy QAM symbols into Log Likelihood Ratios (LLR) for each punctured, coded bit. For the non-iterative receiver, these LLRs are eventually sent to the FEC decoder and bit decisions are made.

For the iterative receiver, there are many more steps before bit decisions are made. Figure 11 shows an iterative receiver based on the turbo principle [8]. The channel matrix H is treated as a rate one linear block code, which is concatenated with the convolutional and Reed-Solomon codes. Iterations are conducted between the spatial demapper and the FEC decoder by passing extrinsic information (i.e., LLRs) back and forth.

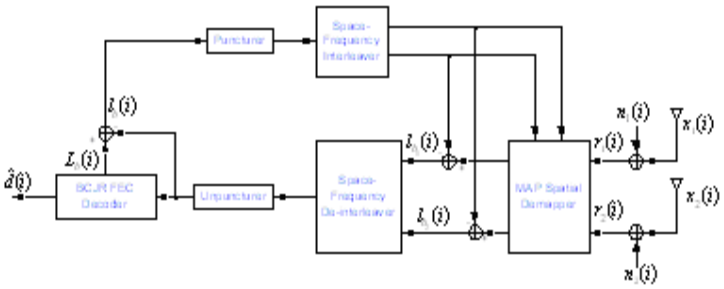

Figure 11: ***Illustration of an iterative receiver***

Performance of this iterative receiver is shown in Figure 12 for 2x2 and 2x3 MIMO architectures. All seven rate modes specified in IEEE 802.16-2004 are used to generate this throughput versus SNR curve. For each architecture, all SIMO subsets such as 1x2 and 1x3 are allowed in the set of possible modulations. For each SNR and each channel realization, all possible combinations of data rate and antenna subsets are run to compute throughput and only the maximum throughput is reported. The maximum throughputs of all channel realizations for that SNR are then averaged and the mean throughput is plotted. The number of iterations for 2x2 MAP curve is 4. The SVD curve includes 2x2 with spatial mode puncturing and 1x2 Maximal Ratio Combining (MRC).

We observe the following:

- 2x2 MAP buys 3-5 dB gain over 2x2 MMSE at higher throughputs.
- 2x2 SVD buys 2-3 dB over 2x2 MMSE at higher throughputs.
- 2x3 MMSE buys 5-7 dB over 2x2 MMSE at higher throughputs.

Therefore we buy the most gain by adding an extra receive chain. This hardware cost can be transferred to base band complexity by using the MAP [9] and BCJR [10] iterative algorithms instead of MMSE, by taking a 1 dB performance hit. The complexity of the MAP spatial demapper is $O(M^K)$, where M is the size of the QAM symbol and K is the number of data streams. This can be rather large for higher order QAMs. We are looking at methods to reduce the complexity of advanced receivers.

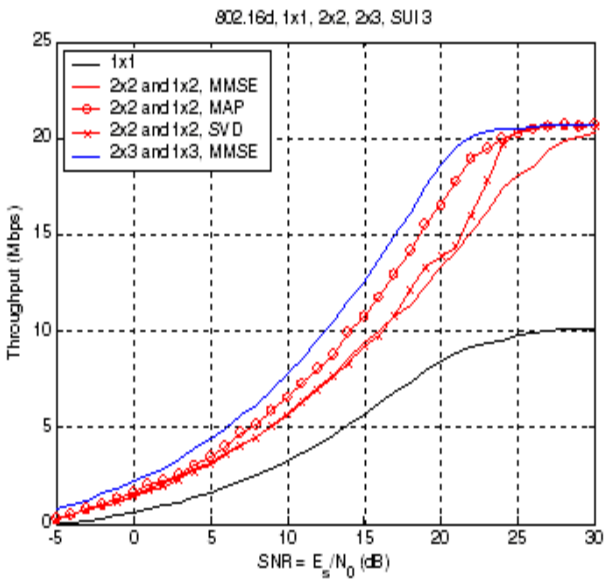

Figure 12: ***Advanced receivers for 2x2 and***

STC AND OTHER STANDARD-COMPLIANT DIVERSITY SCHEMES:

In order to increase the rate and range of the modem, there are several considerations. Generally, the BS can incur more cost and complexity than the SS, so multiple-antenna chains are a good option at the BS, which can then apply receiver diversity techniques. These techniques include switched diversity and maximal ratio combining. To balance the link, the SS needs to have improved performance. Transmission diversity schemes are utilized at the BS that require only one receive antenna at the SS. Two transmit diversity schemes are cyclic delay diversity and Alamouti transmission. We focus on Alamouti transmission.

Alamouti Transmission

The Alamouti transmission scheme is an STC in that it sends information on two transmit antennas and consists of two consecutive transmissions in time. Hence it transmits information in space and time.

In IEEE 802.16-2004 OFDM-256 the Alamouti code is applied to a specific subcarrier index k. For instance, suppose that in the uncoded system $S_1[k]$ and $S_2[k]$ are sent in the first and second OFDM symbol transmissions. The Alamouti encoded symbols send $S_1[k]$ and $S_2[k]$ off the first and second antennas in the first transmission and $-S_2^*[k]$ and $S_1^*[k]$ off the first and second antennas in the next transmission.

The receiver demodulates the received waveform by a few simple operations as follows. Let $Y_1[k]$ and $Y_2[k]$ be the first and second receive OFDM symbols, respectively. Let $C_1[k]$ and $C_2[k]$ be the channel response for the kth subcarrier of the first and second transmit antennas.

$$C_1^*[k]Y_1[k] + C_2[k]Y_2^*[k] = (\| C_1[k] \|^2 + \| C_2[k] \|^2)\hat{S}_1[k] + C_1^*[k]V_1[k] + C_2[k]V_2^*[k]$$

$$C_2^*[k]Y_1[k] - C_1[k]Y_2^*[k] = (\| C_1[k] \|^2 + \| C_2[k] \|^2)\hat{S}_2[k] + C_2^*[k]V_1[k] - C_1[k]V_2^*[k]$$

If the noise $V_1[k]$ and $V_2[k]$ are uncorrelated, then the overall SNR is the maximum achievable and equal to $(\|C_1[k]\|^2+\|C_2[k]\|^2)$(Signal Energy/Noise Energy). Notice that both C 1[k] and C 2[k] need to be in a fade for the overall processed symbol to be in a deep fade. This system has two-fold diversity. For k-fold diversity, the Bit Error Rate (BER) is proportional to $(1/SNR)^k$ in a fading environment.

Alamouti Implementation Details

There are a number of features to IEEE 802.16-2004 OFDM-256 Alamouti transmission that are of interest. The first is that the preamble for Alamouti transmission is transmitted from both antennas with the even subcarriers used for antenna 1 and the odd subcarriers used for subcarrier 2. This means that each set of data needs to be appropriately smoothed, which is done in these simulations. The second is that the pilots have certain degenerate situations: for the first Alamouti transmitted symbol, the pilots destructively add and for the second Alamouti transmitted symbol, the pilots constructively add. Hence, the pilots cannot always be useful. Properly processing the pilot symbols is required. In the simulations, such a technique is used.

We present block diagrams detailing the flow of an Alamouti implementation. This implementation has two parts. The first calculates the parameters that are necessary for data demodulation such as channel estimates. The second part is the actual data demodulation and tracking.

Figure 14 describes the parameter estimation portion. In this part, two channels are estimated, and those channel estimates are used to calculate the Viterbi equalizer coefficients. E_i, is the average energy of the *i*th transmit path. This is a computationally intensive portion of the Alamouti reception; however, it is a one-time computation per burst, so is feasible.

Alamouti Performance Simulations

For the purposes of simulations, three scenarios are simulated each of which are important to typical system vendors. The first set uses an AWGN channel that is the baseline for performance results. In AWGN, BER is the most important

metric. The second set of simulations uses a frequency selective channel normalized so that its average SNR is equal to the instantaneous SNR. These simulations show the performance in frequency selective channels. In fixed wireless scenarios, the receive SNR does not change rapidly, so the average BER during multiple instantiations of the channel is of interest. Finally, in the third set of simulations, the channel is fading. In non-mobile situations, the fading rate is slow, so it is of interest to determine how often the system does not provide good performance. The Packet Error Rate (PER) is a good metric. A fixed-point model of the Alamouti scheme is simulated under the following conditions:

- Full bandwidth IEEE 802.16-2004 OFDM-256
- Stanford University Interim (SUI)-3 model
- 3.5 MHz bandwidth
- Varying SNR
- No timing/frequency offset or drift

All the blocks in Figure 13 are executed. The results are shown in Figures 14 .

The 3 dB theoretical gain, as indicated by Equation 2, is not met at BER=10^{-3}. We expect that at lower BERs, the curves will be closer to expected theoretical gains.

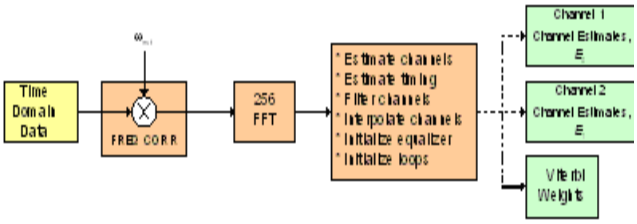

Fig 13: ***Alamouti parameter estimation***

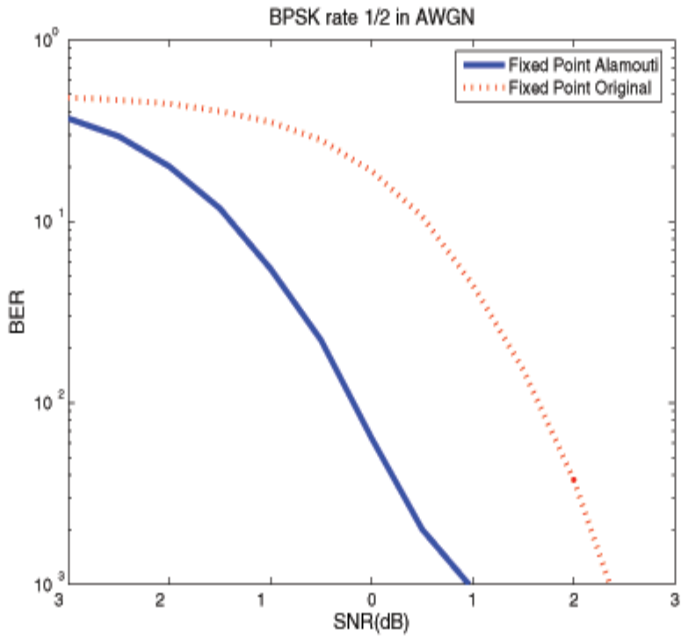

Figure 14: ***BER vs. SNR(dB) for BPSK rate ½***

CONCLUSION

We describe the Physical (PHY) layer of the general communication system. The performance of the PHY layer is strongly correlated to the overall system performance. However, higher-level entities such as Automatic Request (ARQ) for retransmission can also impact system performance. Coding the transmitted signal across antennas, OFDM symbols, and frequency tones,These simulation results assume ideal channel estimation, channel estimate smoothing, and perfect synchronization. Thus, improved gain and QoS is achieved at no cost in bandwidth or transmits power.

REFERENCE

[1]Frank Ohrtman, "WiMAX Handbook", McGraw-Hill Communications Companies, 2005

[2]Jeffrey G. Andrews, Arunabha Ghosh, Rias Muhamed, "Fundamentals of WiMAX", PearsonEducation, February 2007
[3]Y. Ahmet Sekercioglu, Milosh Ivanovich, Alper Yegin, "A survey of MAC based QoS implementations for WiMAX networks", Computer Network(2009)
[4]R. Farhadi, V. T. Vakili, and S. S. Moghadam, "A comparative study of scheduling algorithms for OFDMA-based WiMAX networks," 2011 IEEE 3rd International Conference on Communication Software and Networks, no. Cid, pp. 355–359, 2011.
[5]R. Jain, and a K. Tamimi, "Scheduling in IEEE 802.16e mobile WiMAX networks: key issues and a survey," IEEE Journal on Selected Areas in Communications, vol. 27, no. 2, pp. 156–171, 2009.
[6]Chou, "Two-Tier Scheduling Algorithm for Uplink Transmissions in IEEE 802.16 Broadband Wireless Access Systems," 2006 International Conference on Wireless Communications Networking and Mobile Computing, pp. 6–9, 2006.
[7]Kim, Seungwoon and Yeom, Ikjun, "TCP-aware Uplimk scheduling for IEEE 802.16". IEEE Communication Letter, Feb., 2007.
[8]Zeynep Yurdakul, Sema Oktug, "A Hierarchical Channel-Aware Uplink Scheduler For WiMAX Based Stations", 2010 Sixth Advanced International Conference on Telecommunications, IEEE computer societ y, pp. 398-403.
[9]E. Limouchi, S. T. Branch, A. Salajeghe, M. Pourmina, and A. Zehni, "An Intra-Class Channel-Aware Scheduling in IEEE," Network, IEEE, vol. 1, no. 8, pp. 323–325, 2011.
[10]D. Astely, E. Dahlman, a Furuskar, Y. Jading, M. Lindstrom, and S. Parkvall, "LTE: the evolution of mobile broadband," IEEE Communications Magazine, vol. 47, no. 4, pp. 44–51, 2009.
[11]P. Development and T. Challenges, "Agilent 3GPP Long Term Evolution : System Overview, Product Development and Test Challenges," 2009.
[12]M. Alasti and B. Neekzad, "Quality of Service in WiMAX and LTE Networks,"Communications Magazine, IEEE, vol. 48, no. May, pp. 104–111, 2010.
[13]F. D. Calabrese, C. Rosa, M. Anas, P. H. Michaelsen, K. I. Pedersen, P. E. Mogens "Adaptive Transmission Bandwidth Based Packet Scheduling for LTE Uplink", Nokia Siemens Networks, Denmark
[14]T.E. Kolding, "QoS-Aware Proportional Fair Packet Scheduling with Required Activity Detection", IEEE 64th Vehicular Technology Conference, September 2006.
[15]Sunggu Choi, Kyungkoo Jun, Yeonseung Shin, Seokhoon Kang, Byoungjo Choi. "MAC Scheduling Scheme for VoIP Traffic Service in 3G LTE" Vehicular Technology Conference, 2007.VTC-2007 Fall. 2007 IEEE 66th, 1441—1445
[16]M. Anas, C. Rosa, F. D. Calabrese, K. I. Pedersen, and P. E. Mogensen, "Combined Admission Control and Scheduling for QoS Differentiation in LTE Uplink," 2008 IEEE 68th Vehicular Technology Conference, vol. 68, no. September, pp. 1–5, 2008."
[17]K. Etemad and I. Corporation, "Overview of Mobile WiMAX Technology and Evolution,"Communications magazine, IEEE, vol. 46, no. October, pp. 31–40, 2008.
[18]3GPP, "3GPP System Architecture Evolution: Report on Technical Options and Conclusions(Release 8)", TR 23.882.V8.0.0(2008-09) [19]3GPP TS 36.300 V8.4.0(2008-03)
[20]Fan Wang et al., "Mobile WiMAX Systems: Performance and Evolution", IEEE Communications Magazine, Volume 46, No.10, October 2008
[21]L. Li and S. Shen, "End-to-End QoS Performance Management Across LTE Networks," Network Operations and Management Symposium (APNOMS), 2011 13th Asia-Pacific, vol. 2011, pp. 1–4, 2011.
[22] Zeeshan Ahmed, "Quality of Service in WiMAX for Multimedia Services", Phd thesis, June 2013
[23]Lee Breslau, Deborah Estrin, Kevin Fall, Sally Floyd, John Heidemann, Ahmed Helmy, Polly Huang, Steven McCanne, Kannan Varadhan, Ya Xu, et al. "Advances in network simulation. Computer", 33(5):59–67, 2000. 124,125
[24]Matlab Simulator. 5.0, matlab 5 users guide scalable network technologies.Inc 2010, 2010. 126, 128, 224
[25]V.S. Abhayawardhana, I.J. Wassell, D. Crosby, M.P. Sellars, and M.G. Brown, "Comparison of empirical propagation path loss models for fixed wireless access systems", in Vehicular Technology Conference, Spring 2005, Volume 1, pp. 73–77, 30 May – 1 June 2005.
[26]V. Erceg, L.J. Greenstein, S.Y. Tjandra, S.R. Parkoff, A. Gupta, B. Kulic, A.A. Julius, R.Bianchi, "An Empirically Based Path Loss Model for Wireless Channels in Suburban Environments", in IEEE Journal on Selected Areas in Communications, Volume 17, No. 7, July 1999.
[27]M.J. Feuerstein, K.L. Blackard, T.S. Rappaport, S.Y. Seidel, H.H. Xia, "Path loss, Delay Spread, and Outage Models as Functions of Antenna Height for Microcellular System", in IEEE Transactions on Vehicular Technology, Vol. 43, No 3, pp. 487-498, August 1994.
[28]G.D. Durgin, T.S. Rappaport, and H. Xu, "Measurements and Models for Radio Path Loss In and Around Homes and Trees at 5.85 GHz", in IEEE Transactions on Communications, Volume 46, No 11, pp. 1484–1496, November 1998.

[29]J.W. Porter, I. Lisica, G. Buchwald, "Wideband mobile propagation measurements at 3.7 GHz in an urban environment", in IEEE Antennas and Propagation Society International Symposium,Volume 4, pp. 3645–3648, 20-25 June 2004.

[30]T. Rautiainen, K. Kalliola, J. Juntunen, "Wideband radio propagation characteristics at 5.3 GHz in suburban environments", in Proc. IEEE 16th International Symposium on Personal, Indoor and Mobile Radio Communications, 2005, PIMRC 2005, Volume 2, pp. 868–872, 11–14 September.

